Electronic Supplementary Material (ESI) for CrystEngComm.

In-situ Raman Study of the Crystallization of Glycine

Jingjing Wang[1], Adriana Alieva[1], Matthew Boyes[1], Andrew J. Pollard[2], Cinzia Casiraghi[1*]

[1] Department of Chemistry, University of Manchester, Manchester, M13 9PL, United Kingdom;

[2] National Physical Laboratory, Teddington, Middlesex, TW11 0LW, United Kingdom

* Corresponding author: cinzia.casiraghi@manchester.ac.uk

Supplementary Information

S1 Crystallization Setup

Figure S1 shows the crystallization experiments setup used in this study. The crystallization experiments were carried out as following: a clean silicon substrate covered with an oxide layer (Si/SiO_2) was first placed in a plastic sample box, then a droplet of an undersaturated aqueous glycine solution (2 μL) was deposited on the Si/SiO_2 substrate. The box was partially covered by a glass cover slide, leaving ~1 mm gap around two of the edges, in order to slow down the evaporation rates, thus allowing sufficient time to collect an acceptable Raman signal for fitting purposes. All experiments were carried out in a temperature regulated room at 21 °C.

Under these experimental conditions, the average crystallization time from ten crystallization experiments of glycine solution in H_2O and in D_2O was found to be ~23 and ~29 minutes, respectively, with a range of ~2-3 minutes for both solvents. It must be noted that all times are qualitative as crystallization times, defined as observation of the first crystal, was achieved by eye.

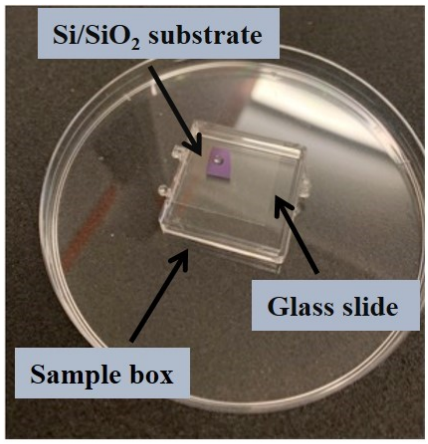

Figure S1 Image of the experimental setup.

S2 Raman spectroscopy

S2.1 Polymorph Distribution

A total of 50 point measurements of the crystals in the centre and at the edges of the triple contact region were taken in order to identify the polymorph distribution. The measurements were taken with a 20X objective, 2400 grooves/mm grating and using less than 5 mW laser power on the sample.

Figure S2.1 shows representative spectra taken at the centre and edge regions of glycine crystals formed from evaporation of H_2O. Based on the CH modes positions,[1] our results indicate that the crystals at the centre of the product are α-glycine; at the edge, the β-polymorph was more prominent (~76 %, of the measurements match with the β-polymorph, while the remaining give α-glycine), in agreement with results previously obtained by our group.[2] Similar results were found for crystals evaporated from D_2O, as shown in Figure S2.2c and Figure S2.2d.

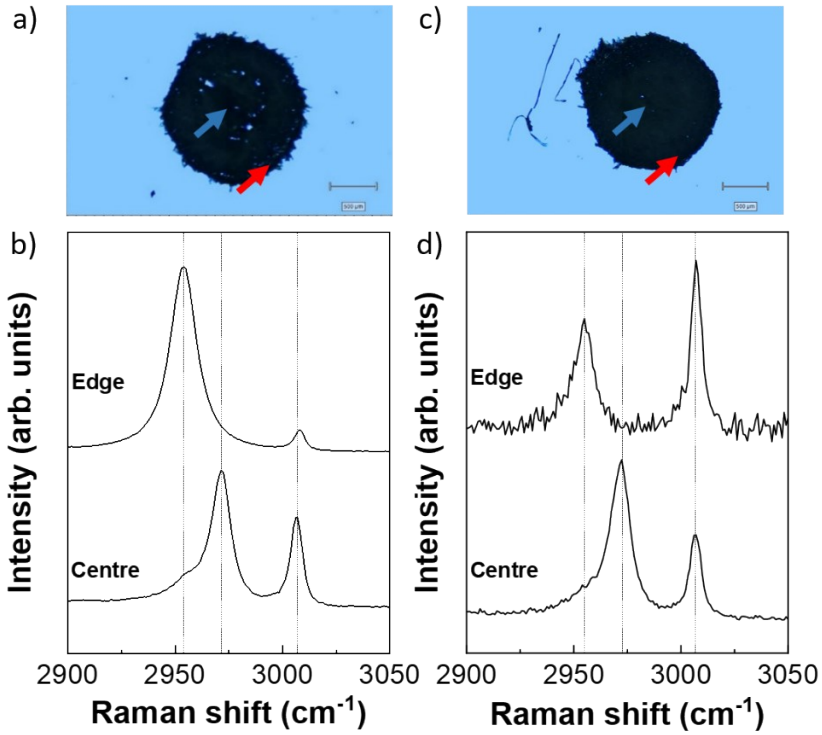

Figure S2.1 a) Optical image of glycine crystals obtained from evaporation of H_2O. b) Representative Raman spectra of glycine crystals measured at the centre (blue arrow) and at the edge region (red arrow) of the droplet. c) Optical image of glycine crystals obtained from evaporation of D_2O. d) Representative Raman spectra of glycine crystals measured at the centre (blue arrow) and at the edge region (red arrow) of the droplet.

S2.2 Raman spectroscopy of Glycine crystallization - Edge region

S2.2.1 Crystallizations in H_2O

10 separate crystallizations from freshly prepared solutions were performed, all under the same conditions as previously mentioned. Figure S2.2 shows representative Raman spectra of the CH region

for each crystallization, in particular at the liquid to solid transition. In all cases, a splitting of the peak before the crystal is formed is observed. Table S1 summarises the results of analysing the positions of both the symmetric and asymmetric stretches, ν_s(CH) and ν_{as}(CH), respectively, during the evaporation of the solvent and eventual crystallization of glycine.

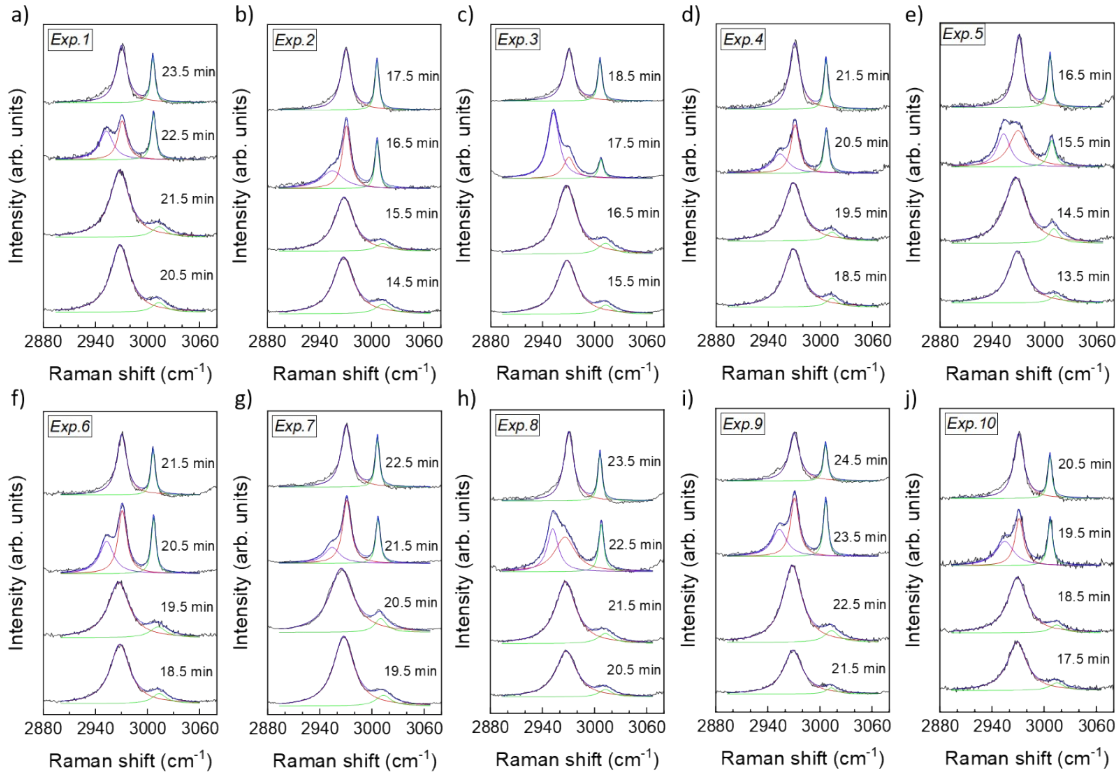

Figure S2.2 Representative Raman spectra of the CH region of glycine crystallizing from H_2O measured at the edges of the droplets, during the transition from liquid to solid state.

Table S1. Summary of the CH peak positions of the Raman spectrum of glycine measured in liquid, solid and at the transition at the edges of the droplet.

Experiment number, solvent	Liquid; Position (cm^{-1}) & FWHM (cm^{-1})	Solid; Position (cm^{-1}) & FWHM (cm^{-1})	Transition; Position (cm^{-1}) & FWHM (cm^{-1})
1, H_2O	ν_s(CH) = 2968; 27 ν_{as}(CH) = 3012; 20	ν_s(CH) = 2972; 15 ν_{as}(CH) = 3007; 5	ν_{as}(CH) = 3007; 6 ν_s(CH) = 2971; 12 ν_s(CH) = 2953; 19 Difference = 36;54

2, H_2O	ν_s(CH) = 2968; 26 ν_{as}(CH) = 3011; 29	ν_s(CH) = 2971; 14 ν_{as}(CH) = 3006; 5	ν_{as}(CH) = 3006; 6 ν_s(CH) = 2971; 11 ν_s(CH) = 2954; 30 Difference = 35; 52
3, H_2O	ν_s(CH) = 2968; 28 ν_{as}(CH) = 3012; 20	ν_s(CH) = 2970; 14 ν_{as}(CH) = 3006; 5	ν_{as}(CH) = 3006; 6 ν_s(CH) = 2970; 15 ν_s(CH) = 2954; 22 Difference = 36; 52
4, H_2O	ν_s(CH) = 2967; 27 ν_{as}(CH) = 3010; 17	ν_s(CH) = 2971; 15 ν_{as}(CH) = 3006; 5	ν_{as}(CH) = 3006; 6 ν_s(CH) = 2970; 12 ν_s(CH) = 2954; 22 Difference = 36; 52
5, H_2O	ν_s(CH) = 2968; 30 ν_{as}(CH) = 3010; 15	ν_s(CH) = 2971; 13 ν_{as}(CH) = 3006; 5	ν_{as}(CH) = 3006; 6 ν_s(CH) = 2970; 25 ν_s(CH) = 2954; 18 Difference = 36; 52
6, H_2O	ν_s(CH) = 2968; 29 ν_{as}(CH) = 3010; 22	ν_s(CH) = 2971; 14 ν_{as}(CH) = 3007; 5	ν_{as}(CH) = 3007; 6 ν_s(CH) = 2971; 12 ν_s(CH) = 2953; 19 Difference = 36; 54
7, H_2O	ν_s(CH) = 2966; 32 ν_{as}(CH) = 3012; 16	ν_s(CH) = 2971; 14 ν_{as}(CH) = 3006; 5	ν_{as}(CH) = 3006; 6 ν_s(CH) = 2971; 11 ν_s(CH) = 2954; 21 Difference = 35; 52
8, H_2O	ν_s(CH) = 2966; 28 ν_{as}(CH) = 3012; 21	ν_s(CH) = 2971; 14 ν_{as}(CH) = 3006; 5	ν_{as}(CH) = 3007; 7 ν_s(CH) = 2971; 29 ν_s(CH) = 2954; 17 Difference = 36; 53
9, H_2O	ν_s(CH) = 2967; 31 ν_{as}(CH) = 3013; 21	ν_s(CH) = 2972; 14 ν_{as}(CH) = 3007; 5	ν_{as}(CH) = 3006; 7 ν_s(CH) = 2970; 18 ν_s(CH) = 2954; 22 Difference = 36; 52
10, H_2O	ν_s(CH) = 2968; 27 ν_{as}(CH) = 3013; 20	ν_s(CH) = 2972; 14 ν_{as}(CH) = 3007; 5	ν_{as}(CH) = 3007; 6 ν_s(CH) = 2971; 18 ν_s(CH) = 2954; 24 Difference = 36; 53

AVERAGE, H_2O	v_s(CH) = 2967.4; 28.5 v_{as}(CH) = 3011.5; 20.1	v_s(CH) = 2971.2; 14.1 v_{as}(CH) = 3006.4; 5.0	v_{as}(CH) = 3006.4; 6.2 v_s(CH) = 2970.6; 16.3 v_s(CH) =2953.8; 21.4 Difference = 35.8; 52.6

S2.2.2 Crystallizations in D_2O

10 separate crystallizations from freshly prepared solutions were performed, all under the same conditions as previosuly mentioned. Figure S2.3 shows representative Raman spectra of the CH region for each crystallization, in particular at the liquid to solid transition. In all cases, a splitting of the peak before the crystal is formed is observed. Table S2 summarises the results of analysing the positions of both the symmetric and asymmetric stretches, during the evaporation of the solvent and eventual crystallization of glycine.

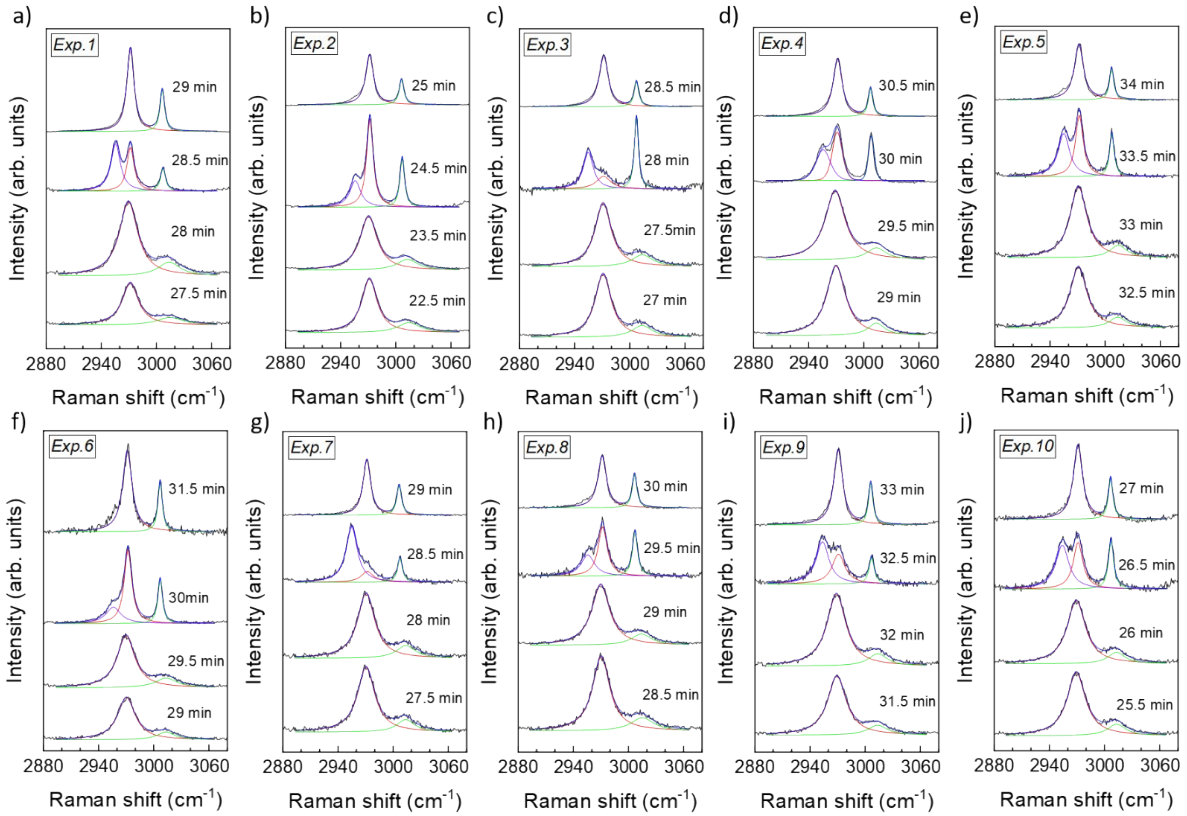

Figure S2.3 Representative Raman spectra of the CH region of glycine crystallizing from D_2O measured at the edges of the droplet, during the transition from liquid to solid state.

Table S2. Summary of the CH peak positions of the Raman spectrum of glycine measured in liquid, solid and at the transition at the edges of the droplet.

Experiment number, solvent	Liquid; Position (cm^{-1}) & FWHM (cm^{-1})	Solid; Position (cm^{-1}) & FWHM (cm^{-1})	Transition; Position (cm^{-1}) & FWHM (cm^{-1})
1, D_2O	ν_s(CH) = 2968; 24 ν_{as}(CH) = 3014; 29	ν_s(CH) = 2971; 9 ν_{as}(CH) = 3006; 5	ν_{as}(CH) = 3007; 6 ν_s(CH) = 2972; 15 ν_s(CH) = 2956; 17 Difference = 35; 51
2, D_2O	ν_s(CH) = 2968; 22 ν_{as}(CH) = 3012; 27	ν_s(CH) = 2972; 10 ν_{as}(CH) = 3006; 4	ν_{as}(CH) = 3007; 6 ν_s(CH) = 2972; 14 ν_s(CH) = 2956; 19 Difference = 35; 51
3, D_2O	ν_s(CH) = 2969; 21 ν_{as}(CH) = 3014; 27	ν_s(CH) = 2971; 12 ν_{as}(CH) = 3007; 6	ν_{as}(CH) = 3007; 5 ν_s(CH) = 2972; 20 ν_s(CH) = 2954; 23 Difference = 35; 53
4 D_2O	ν_s(CH) = 2969; 24 ν_{as}(CH) = 3014; 25	ν_s(CH) = 2972; 12 ν_{as}(CH) = 3007; 5	ν_{as}(CH) = 3007; 5 ν_s(CH) = 2970; 20 ν_s(CH) = 2955; 26 Difference = 37; 52
5, D_2O	ν_s(CH) = 2970; 22 ν_{as}(CH) = 3014; 23	ν_s(CH) = 2972; 12 ν_{as}(CH) = 3007; 5	ν_{as}(CH) = 3007; 6 ν_s(CH) = 2971; 10 ν_s(CH) = 2956; 18 Difference = 36; 51
6, D_2O	ν_s(CH) = 2969; 23 ν_{as}(CH) = 3015; 29	ν_s(CH) = 2971; 12 ν_{as}(CH) = 3007; 6	ν_{as}(CH) = 3007; 6 ν_s(CH) = 2971; 10 ν_s(CH) = 2955; 22 Difference = 36; 52
7, D_2O	ν_s(CH) = 2968; 23 ν_{as}(CH) = 3013; 25	ν_s(CH) = 2971; 10 ν_{as}(CH) = 3007; 6	ν_{as}(CH) = 3007; 6 ν_s(CH) = 2970; 17 ν_s(CH) = 2954; 24 Difference = 37; 53
8, D_2O	ν_s(CH) = 2968; 24 ν_{as}(CH) = 3013; 27	ν_s(CH) = 2971; 11 ν_{as}(CH) = 3007; 6	ν_{as}(CH) = 3007; 7 ν_s(CH) = 2971; 14

			ν_s(CH) = 2955; 20 Difference = 36; 52
9, D_2O	ν_s(CH) = 2968; 25 ν_{as}(CH) = 3013; 25	ν_s(CH) = 2971; 12 ν_{as}(CH) = 3006; 6	ν_{as}(CH) = 3007; 7 ν_s(CH) = 2970; 16 ν_s(CH) = 2954; 19 Difference = 37; 53
10, D_2O	ν_s(CH) = 2969; 24 ν_{as}(CH) = 3013; 23	ν_s(CH) = 2971; 12 ν_{as}(CH) = 3006; 6	ν_{as}(CH) = 3007; 7 ν_s(CH) = 2970; 13 ν_s(CH) = 2954; 19 Difference = 37; 53
AVERAGE, D_2O	ν_s(CH) = 2968.6; 23.2 ν_{as}(CH) = 3013.5; 26.0	ν_s(CH) = 2971.3; 11.2 ν_{as}(CH) = 3006.6; 5.5	ν_{as}(CH) = 3007.0; 6.1 ν_s(CH) = 2970.9; 14.9 ν_s(CH) = 2954.9; 20.7 Difference = 36.1; 52.1

Note that in the case of D_2O, the Raman spectrum shows an additional characteristic peak at 2500 cm^{-1}, associated to D-O stretching vibrations.[3] Figure S2.4 illustrates the evolution of the Raman spectrum of the CH region over time, which includes the peak at 2500 cm^{-1}. This peak disappears after 27 minutes, so it can be used to identify the point at which almost complete evaporation of the solvent occurs, hence confirming the transition from liquid to solid.

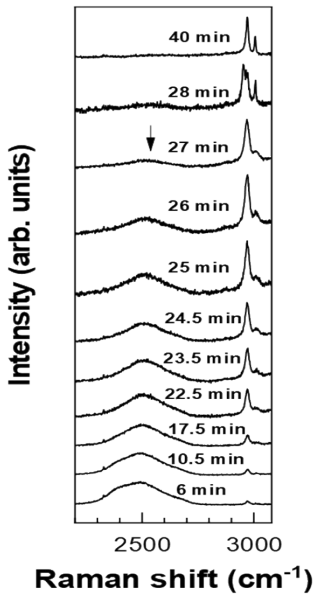

Figure S2.4 Evolution of the CH region of the Raman spectrum of glycine crystallizing from D_2O. The D-O peak, at 2500 cm^{-1}, disappears after 27 minutes, indicating almost complete evaporation.

S2.3 Raman spectroscopy of Glycine crystallization – Centre region

3 separate crystallizations from freshly prepared solutions were performed, all under the same conditions as previoulsy mentioned. Figure S2.5 shows representative Raman spectra of the CH region from each crystallization, in particular at the liquid to solid transition. In all cases, a splitting of the CH peak before the crystal is formed is observed. Table S3 summarises the results of analysing the positions of both the symmetric and asymmetric stretches, during the evaporation of the solvent and eventual crystallization of glycine.

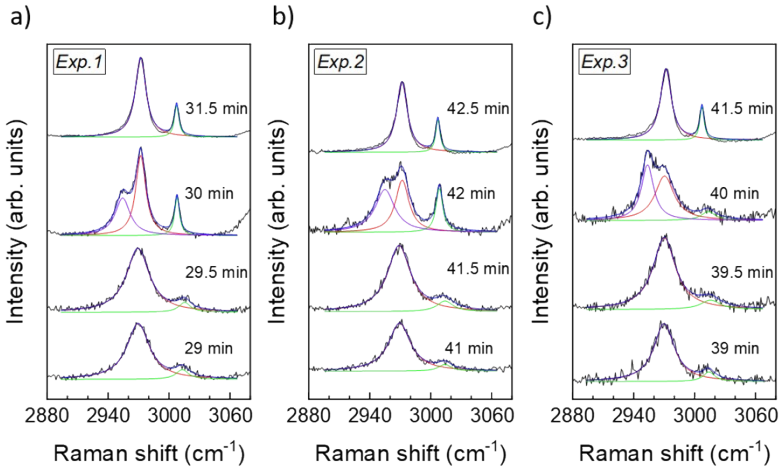

Figure S2.5 Representative Raman spectra of the CH region of glycine crystallizing from H_2O measured at the centre of the droplet, during the transition from liquid to solid state.

Table S3. Summary of the CH peak positions of the Raman spectrum of glycine measured in liquid, solid and at the transition at the centre of the droplet.

Experiment number, solvent	Liquid; Position (cm^{-1}) & FWHM (cm^{-1})	Solid; Position (cm^{-1}) & FWHM (cm^{-1})	Transition; Position (cm^{-1}) & FWHM (cm^{-1})
1, H_2O	ν_s(CH) = 2969; 27 ν_{as}(CH) = 3015; 14	ν_s(CH) = 2972; 12 ν_{as}(CH) = 3007; 6	ν_{as}(CH) = 3007; 5 ν_s(CH) = 2972; 12 ν_s(CH) = 2955; 19 Difference = 35; 52

2, H_2O	ν_s(CH) = 2969; 27 ν_{as}(CH) = 3014; 19	ν_s(CH) = 2972; 13 ν_{as}(CH) = 3007; 5	ν_{as}(CH) = 3007; 8 ν_s(CH) = 2970; 16 ν_s(CH) = 2955; 23 Difference = 37; 52
3, H_2O	ν_s(CH) = 2970; 27 ν_{as}(CH) = 3014; 23	ν_s(CH) = 2972; 13 ν_{as}(CH) = 3007; 5	ν_{as}(CH) = 3007; 7 ν_s(CH) = 2970; 17 ν_s(CH) = 2955; 20 Difference = 37; 52
AVERAGE, H_2O	ν_s(CH) = 2969.3; 27.0 ν_{as}(CH) = 3014.3; 18.7	ν_s(CH) = 2972.0; 12.7 ν_{as}(CH) = 3007.0; 5.3	ν_{as}(CH) = 3007.0; 6.7 ν_s(CH) = 2970.7; 15.0 ν_s(CH) = 2955.0; 20.7 Difference = 36.3; 52.0

Figure S2.6 shows a representative evolution of the CH peak positions, obtained by fitting the Raman spectra, showing the same qualitative behavious as for the measurements obtained at the center region.

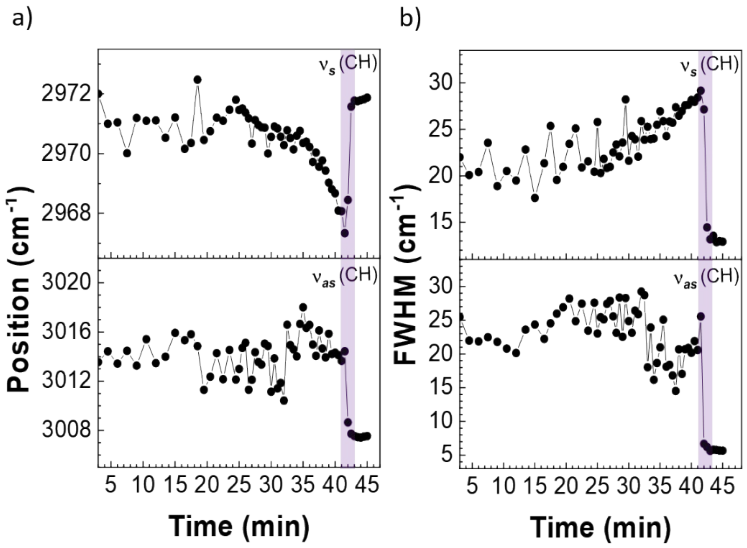

Figure S2.6 a) Peak position and b) FWHM of ν_s(CH) and ν_{as}(CH) as function of the crystallization time. The purple shadow shows the transition from liquid to solid state.

References

1 N. V. Surovtsev, S. V. Adichtchev, V. K. Malinovsky, A. G. Ogienko, V. A. Drebushchak, A. Y. Manakov, A. I. Ancharov, A. S. Yunoshev and E. V. Boldyreva, *J. Chem. Phys.*, 2012, **137**, 065103.

2 M. Boyes, A. Alieva, J. Tong, V. Nagyte, M. Melle-Franco, T. Vetter and C. Casiraghi, *ACS Nano*, 2020, **14**, 10394–10401.

3 K. Furić, V. Mohaček, M. Bonifačić and I. Štefanić, *J. Mol. Struct.*, 1992, **267**, 39–44.